Optics Letters

Hyperspectral infrared laser polarimetry for single-shot phase–amplitude imaging of thin films

Andreas Furchner,[1,*] Christoph Kratz,[1] Jörg Rappich,[2] and Karsten Hinrichs[1]

[1]Leibniz-Institut für Analytische Wissenschaften—ISAS—e. V., Schwarzschildstraße 8, 12489 Berlin, Germany
[2]Helmholtz-Zentrum Berlin für Materialien und Energie GmbH, Institut für Silizium-Photovoltaik, Kekuléstraße 5, 12489 Berlin, Germany
*Corresponding author: andreas.furchner@isas.de

Received 8 August 2019; revised 29 August 2019; accepted 29 August 2019; posted 29 August 2019 (Doc. ID 374975); published 1 October 2019

We recently presented a novel laser-based infrared (IR) spectroscopic phase–amplitude polarimeter for sub-decisecond and sub-mm^2 measurements of organic thin films [Opt. Lett. 44, 4387 (2019)]. Here we report on the hyperspectral-imaging capabilities of this device. The single-shot polarimeter employs a broadly tunable mid-IR (1318–1765 cm^{-1}) quantum cascade laser (QCL) and a four-channel beam-division design for simultaneous phase and amplitude measurements. Fast QCL tuning speeds of up to 1500 cm^{-1}/s enable hyperspectral mapping of large sample areas (50 × 50 mm^2) within several tens of minutes, achieving 120 µm spatial and <0.5 cm^{-1} spectral resolution. We apply the instrument for imaging both the heterogeneous chemical and structural properties of sub-100 nm thin polymer and fatty-acid films. Our polarimeter opens up new applications regarding laterally resolved IR analyses of complex thin films.

https://doi.org/10.1364/OL.44.004893

IR and Raman spectroscopy are widely known for their ability to correlate measured spectra with chemical and structural sample properties [1]. Defined sample mapping renders such vibrational spectroscopies highly appealing for studies of heterogeneous surfaces, such as functional coatings, biological samples, and organic semiconductor surfaces. Polarization-sensitive imaging is particularly attractive for investigating thin films and anisotropic surfaces, as it can obtain both amplitude and phase information. However, classical laboratory spectroscopy based on the Fourier-transform (FT-IR) technique imposes strong restrictions regarding time, spatial and spectral resolution, as well as ambient stability, when aiming for thin-film sensitivity in short mapping times.

To tackle these drawbacks, we present a novel IR polarimeter that combines a brilliant laser source with an ellipsometric single-shot concept. The instrument uses a tunable quantum cascade laser (QCL) that provides the necessary brightness for sensitive, laterally highly resolved imaging of thin organic films. The single-shot design enables simultaneous measurements of four different polarization states, from which complementary ellipsometric phase and amplitude information [2,3] related to thickness and structural, chemical, and optical sample properties are derived.

In a prior two-channel detection approach [4], we achieved time resolutions of 60 ms per wavelength. Amplitude maps of 50 × 50 = 2500 spots with lateral steps of 100 µm were feasible in less than 10 min, albeit at only mm^2 spatial resolution and for just a single wavelength. With only two detection channels, additional single-wavelength phase maps led to a substantial increase in acquisition times. Spectral maps were possible only in a step-and-scan mode, which resulted in unacceptable time requirements of several days per measurement.

With the novel design presented here, measurement times decrease drastically to currently 16 µs per wavelength, to <100 ms for a 150 cm^{-1} spectral sweep, and to $\mathcal{O}$(10 min) for large-scale simultaneous hyperspectral imaging of *both* amplitude and phase. An area of 1 mm^2 containing 32 spots in lateral steps of 250 × 125 µm^2 can be mapped in well under 1 min.

In a previous Letter [5], we detailed the technical aspects of the instrument and showed applications regarding single-spot, sub-second, real-time phase–amplitude monitoring of a thermo-induced thin-film phase transition. Here we will focus on the hyperspectral-imaging capabilities of the device.

Hyperspectral images consist of complete spectral, polarimetric phase–amplitude data at each measured spot on the sample. In other words, the data span a five-dimensional hypercube containing the laser spot's X and Y coordinates in the cube's first two dimensions, spectral information along its third dimension, and phase and amplitude values along its fourth and fifth dimension. The information richness of such spatiospectral polarimetric data enables unprecedented comprehensive laterally resolved thin-film IR analysis regarding structure, morphology, chemistry, composition, interactions, optical anisotropy, etc.

We present hyperspectral imaging data of two sample systems. The first is a laterally chemically uniform, but topographically inhomogeneous, film of poly(*N*-isopropylacrylamide) [PNIPAAm], a widely used stimuli-responsive polymer in biosensors [6] and smart coatings [7]. The second is a both chemically and structurally heterogeneous film of myristic acid [MyA], a fatty acid with applications in biomedicine [8] and phase-change materials for energy storage [9].

The polarimeter (Sentech Instruments GmbH) is depicted schematically in Fig. 1. It comprises an external-cavity QCL (MIRcat 2100, Daylight Solutions), a 50 × 50 mm^2 mapping stage, CaF_2 micro-focus lenses for spot sizes of 280 × 120 µm^2 (at 65° incidence angle), and a four-faceted gold-pyramid beam

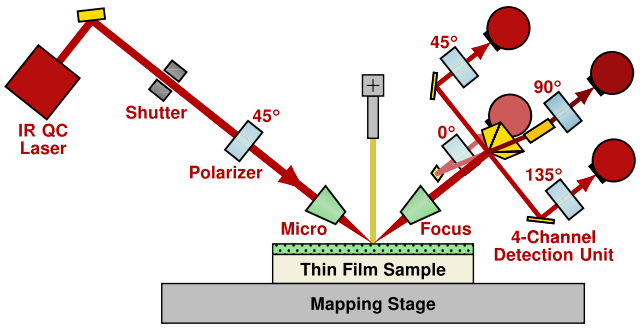

Fig. 1. Schematic of the single-shot IR imaging polarimeter.

splitter followed by a four-channel detection unit with photovoltaic InAsSb detectors (P13894-211, Hamamatsu). The channels contain KRS-5 polarizers (0.25 μm wire-grid spacing, polarization degree >99.6%, Specac Ltd.) at fixed azimuths of 0°, 45°, 90°, and 135°, rendering the polarimeter an IR ellipsometer after Röseler's four-intensity scheme [10] to derive the ellipsometric ratio

$$\varrho = \tan\Psi \cdot e^{i\Delta} = r_p/r_s \tag{1}$$

from a synchronized single-shot intensity measurement of

$$\cos 2\Psi = \frac{I_{90°} - I_{0°}}{I_{90°} + I_{0°}}, \quad \sin 2\Psi \cos\Delta = \frac{I_{45°} - I_{135°}}{I_{45°} + I_{135°}}. \tag{2}$$

The ellipsometric parameters $\tan\Psi$ and Δ are the amplitude ratio and phase difference between the complex reflection coefficients parallel (p) and perpendicular (s) to the plane of incidence. Further details on set-up, laser, and detection electronics are given in [5].

We now apply the polarimeter to the hyperspectral imaging of heterogenous thin films on gold substrates. Measurements were performed in lateral steps of 250 μm along the plane of incidence (X) and 125 μm perpendicular to it (Y). All spectra were recorded between 1318.5–1764.0 cm^{-1} in sub-0.02 cm^{-1} sampling intervals, and subjected to low-pass and moving-average filters to obtain an effective spectral resolution of 4 cm^{-1}. Band amplitudes were quantified as the ratio between $\tan\Psi$ on and off the band (e.g., $\tan\Psi_{1661/1708} = \tan\Psi_{1661}/\tan\Psi_{1708}$).

Figure 2 shows large-scale phase and amplitude maps, as well as linescans and ellipsometric spectra, of a structured PNIPAAm thin film. The sample surface, originally covered by a uniform spin-coated layer, was restructured by pipetting three separated drops of water onto the non-covalently bonded, water-soluble film. Upon water evaporation, the polymer has accumulated into three strongly heterogeneous islands with thicknesses of some 100 nm. The top-left region of the substrate remains partially coated with a thin film of average thickness of 95 nm.

As a secondary amide, PNIPAAm gives rise to amide I and II bands, associated with vibrational modes of its amide (HNCO) side groups, as well as to several alkyl-related (CH_x) bands from polymer backbone and side groups [11]. Amide bands typically comprise multiple components that provide insights into intra- and intermolecular interactions, such as the secondary structure of proteins, or the various amide–amide and amide–water hydrogen-bond patterns of PNIPAAm [12].

The strong phase contrast ($\cos\Delta$) in Fig. 2(a), mapped beside vibrational absorption bands at 1750 cm^{-1}, identifies the different homogeneous and inhomogeneous film areas. The phase is directly related to film thickness, as its baseline follows the Fabry–Pérot oscillations inside the layer. In the light-colored regions, where the substrate is not covered with any adlayer, $\cos\Delta$ is expectedly close to −1, because gold behaves almost like an ideal IR reflector. Larger $\cos\Delta$ values in the darker-colored areas are associated with an increasingly thick polymer layer.

The amplitude contrast ($\tan\Psi$) of vibrational absorption bands provides chemical sample information. Values close to 1 represent uncoated regions, whereas smaller values reveal the presence of material with a specific vibrational absorption. For instance, the alkyl-bending band map at 1366 cm^{-1} is sensitive to any deposited organic material that exhibits such $\delta(CH_x)$-related vibrational modes, meaning PNIPAAm itself but also adsorbed contaminants. Therefore, film, the three islands, and multiple small-sized spots appear in the image. A non-specific $\tan\Psi$ map at 1720 cm^{-1} shows only the three islands, as it is much less influenced by small thicknesses.

A $\tan\Psi$ amplitude map of PNIPAAm's amide I band at 1661 cm^{-1} is depicted in Fig. 2(b). Such slices of the hyperspectral data cube can be used for studying local changes in molecular interactions, which would lead to a modified amide band envelope [12]. The image highlights the device's sub-mm^2 spatial resolution. Even very small structures, such as the thin rings of polymer surrounding the thicker islands, are laterally resolved.

To investigate molecular interactions and homogeneity in more detail, a linescan over the film in the top-left sample area is presented in Fig. 2(c). Spectra of the uncoated gold regions are featureless, whereas those of the PNIPAAm layer are dominated by its amide I and II bands. As a spin-coating artifact, the polymer film exhibits thickness fluctuations of a few nm over lateral distances in the 100 μm range. However, there is no substantial variation in the amide band composition [12], indicating spatial homogeneity of amide–amide interactions across the film.

While this sample is chemically uniform and shows no obvious alterations in molecular interactions, the data demonstrate the potential of hyperspectral IR polarimetry for in-depth, spatially resolved sample investigations, potentially for secondary-structure analysis of thin protein and biorelated films, but also for homogeneity studies of functional thin films and coatings.

The next example is a drop-cast thin film of MyA [5] that was chemically altered from its pure form to a complexed-like state by partially exposing it to NaOH in ethanol (EtOH). Figure 3(a) shows various phase and amplitude maps obtained from a hyperspectral measurement. Again, the $\cos\Delta$ map provides topography information. An EtOH drop and a NaOH + EtOH drop were placed onto the originally circular-shaped MyA film at X = 11 mm and 14 mm, respectively, leading to a NaOH concentration gradient in the intermixing area. Due to the lack of surface tension of ethanol, the two droplets spread over time and dissolved most of the MyA. Complexation of MyA occurred in areas with sufficient amounts of NaOH. After ethanol evaporation, the optical thickness—i.e., film thickness times refractive index—as measured by the phase map, dropped substantially in those modified areas; hence $\cos\Delta$ is closer to −1.

Different domains of pure MyA and complexed MyA are sensitively sensed in the amplitude maps of the two marker bands at 1706 cm^{-1} and 1379 cm^{-1}, respectively, which

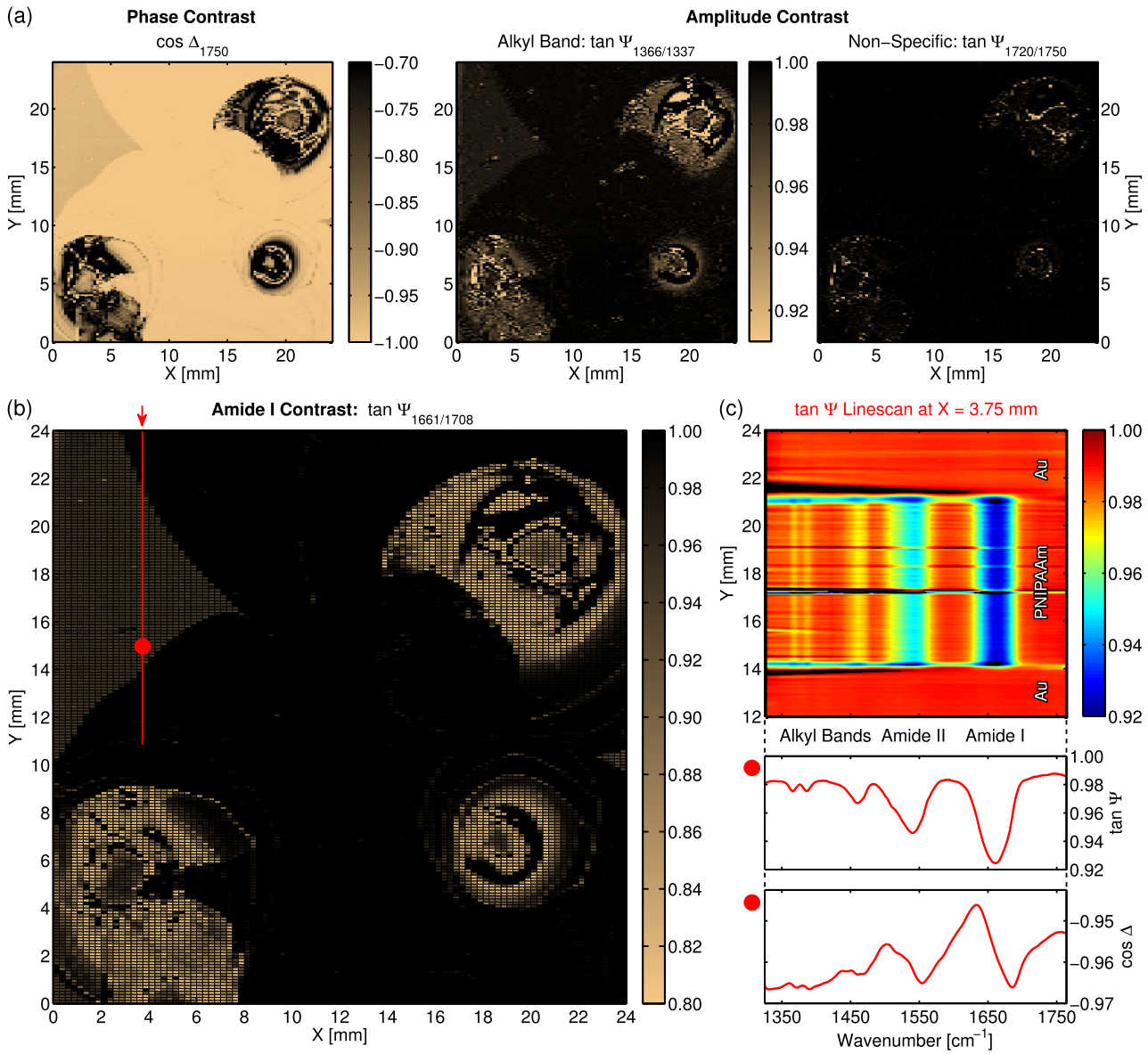

Fig. 2. Hyperspectral data of a structured PNIPAAm thin film on Au. (a) Polarimetric phase and amplitude maps at different wavelengths. (b) Amide I band amplitude map. (c) tan Ψ linescan with selected ellipsometric spectra of the homogeneous layer.

distinguish the two states, as will be discussed later in more detail. After ethanol evaporation, pure MyA remained only in a small area reminiscent of a crescent moon. Complexed MyA developed in a beetle-shaped area around $(X, Y) = (13, 8)$ mm.

A detailed multispectral image of the chemical contrast between pure and complexed MyA is depicted in Fig. 3(b). It demonstrates how both compositional and structural information are accessible, especially obvious in the areas of complexed MyA, highlighting the potential of hyperspectral IR polarimetry for laterally resolved chemical and structural film analysis.

Another layer of detail is given in Fig. 3(c) in form of a linescan across the sample. It reveals the different vibrational characteristics in the region of pure MyA (A), an intermediate area (B), and the region of complexed MyA (C). The variations in band intensities indicate that pure MyA is adsorbed to the substrate with hardly any structural heterogeneity, whereas complexed MyA covers the surface in vastly varying amounts. Having access to spectral information is essential for identifying chemical and structural properties. Pure and complexed MyA exhibit distinct vibrational spectra. Pure MyA features an intense band at 1706 cm^{-1}, associated with the ν(C=O) stretching mode of the fatty acid's protonated COOH carboxyl groups, as well as numerous bands between 1318–1500 cm^{-1}, related mainly to modes of MyA's saturated aliphatic chains. The prominent ν(C=O) band is absent in the complexed MyA, which rather shows two less intense bands at 1554 cm^{-1} and 1617 cm^{-1}, probably from the $\nu(COO^-)$ modes of deprotonated carboxyl groups. Moreover, several intense bands appear at lower wavenumbers, which enable straightforward chemical discriminability of complexed from pure MyA. As shown above, the bands at 1706 cm^{-1} and 1379 cm^{-1} were successfully used as proxies for pure and complexed MyA. More detailed band

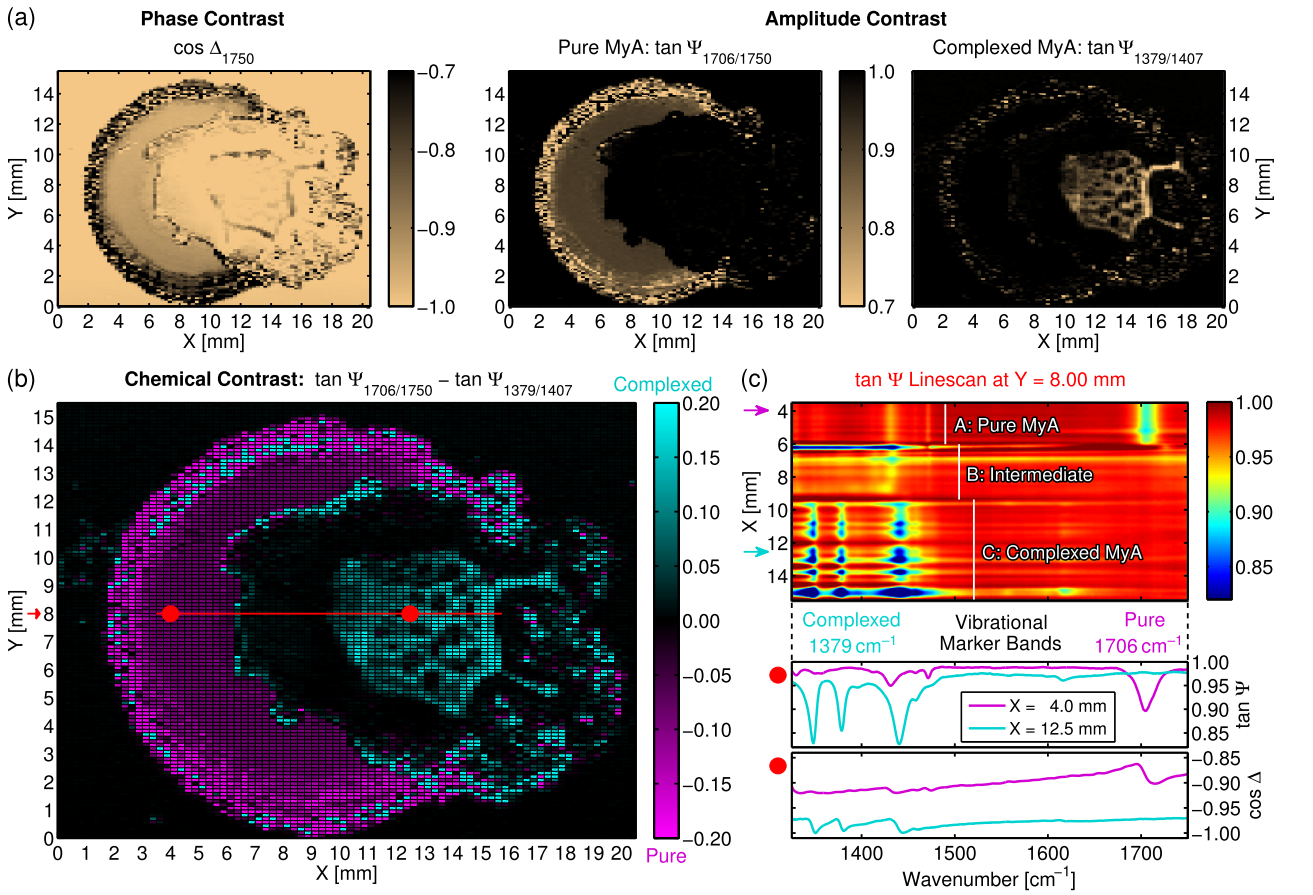

Fig. 3. Hyperspectral data of a structured, partially chemically modified MyA thin film on Au. (a) Polarimetric phase and amplitude maps at different wavelengths, characteristic for topography, pure and complexed MyA. (b) Chemical-contrast map showing the predominant areas of pure and complexed MyA. (c) tan Ψ linescan with selected ellipsometric spectra and marker bands.

assignments and studies of the complexation process are the subject of future investigations.

The wealth of information obtained from a hyperspectral measurement facilitates complex thin-film analyses and opens the door to a plethora of new applications, such as comprehensive process and quality control; rheology, relaxation, and related studies; and analysis of structured, anisotropic films and biological surfaces. We currently work on coupling microfluidic flow cells to the instrument in order to image solid–liquid interfaces, as well as functional, sensor and biocompatible surfaces, with unparalleled spatial resolution. The wide, accessible spectral range is highly relevant for such applications, as it enables measurements of, e.g., lipids, peptides, proteins, polymers, and membranes. The instrument's four polarization-detection channels can also be tailored for imaging other specific polarimetric properties, such as circular dichroism, associated with the film's Mueller matrix. Improving certain technical device aspects might push imaging times into the sub-minute range, which would allow for time-resolved imaging of kinetic processes.

Funding. Ministerium für Innovation, Wissenschaft und Forschung des Landes Nordrhein-Westfalen; Bundesministerium für Bildung und Forschung; European Regional Development Fund (EFRE 1.8/13); Regierender Bürgermeister von Berlin—Senatskanzlei Wissenschaft und Forschung.

Acknowledgment. The instrument was designed and set up in close collaboration with Sentech Instruments GmbH. We particularly thank U. Richter, G. Dittmar, K. Schreiter, F. Günther, M. Hofmann, and J. Reck for support; M. Godejohann (MG Optical Solutions) for help with laser and boxcar electronics; I. Engler and Ö. Savas (ISAS Berlin) for technical assistance; and S. Rauch and K.-J. Eichhorn (IPF Dresden) for fruitful discussions.

REFERENCES

1. P. Larkin, *Infrared and Raman Spectroscopy* (Elsevier, 2011).
2. M. Losurdo and K. Hingerl, *Ellipsometry at the Nanoscale* (Springer, 2013).
3. K. Hinrichs and K.-J. Eichhorn, *Ellipsometry of Functional Organic Surfaces and Films* (Springer, 2018).
4. A. Furchner, C. Kratz, D. Gkogkou, H. Ketelsen, and K. Hinrichs, Appl. Surf. Sci. **421**, 440 (2017).
5. A. Furchner, C. Kratz, and K. Hinrichs, Opt. Lett. **44**, 4387 (2019).
6. M. R. Islam, A. Ahiabu, and M. J. Serpe, Sensors **14**, 8984 (2014).
7. B. D. Ratner and S. J. Bryant, Annu. Rev. Biomed. Eng. **6**, 41 (2004).
8. J. M. Silva, S. Akkache, A. C. Araújo, Y. Masmoudi, R. L. Reis, E. Badens, and A. R. C. Duarte, Mater. Sci. Eng. C **99**, 599 (2019).
9. K. Pielichowska and K. Pielichowski, Prog. Mater. Sci. **65**, 67 (2014).
10. A. Röseler and E.-H. Korte, in *Handbook of Vibrational Spectroscopy*, J. M. Chalmers and P. R. Griffiths, eds. (Wiley, 2006).
11. Y. Maeda, T. Higuchi, and I. Ikeda, Langmuir **16**, 7503 (2000).
12. A. Furchner, A. Kroning, S. Rauch, P. Uhlmann, K.-J. Eichhorn, and K. Hinrichs, Anal. Chem. **89**, 3240 (2017).